Journal of Geophysical Research (Oceans)

Supporting Information for

Net submarine groundwater-derived dissolved inorganic nutrients and carbon input to the stratified karstic estuary of the Krka River (Adriatic Sea, Croatia)

Jianan Liu[1], Enis Hrustić [2,3], Jinzhou Du[1,*], Blaženka Gašparović[4], Milan Čanković[4], Neven Cukrov[4], Zhuoyi Zhu[1], and Ruifeng Zhang[1,5]

[1] State Key Laboratory of Estuarine and Coastal Research, East China Normal University, 500 Dongchuan Rd.,Shanghai 200241, PR China

[2] Institute for marine and coastal research, University of Dubrovnik, Kneza Damjana Jude 12, 20000 Dubrovnik, Croatia

[3] Center for marine research, Ruđer Bošković Institute, Giordano Paliaga 5, 52210 Rovinj, Croatia

[4] Division for Marine and Environmental Research, Ruđer Bošković Institute, Bijenička cesta 54, 10000 Zagreb, Croatia

[5] Institute of Oceanology, Shanghai Jiao Tong University, 800 Dongchuan RD, Shanghai 200240, PR China

Contents of this file

Introduction

This supporting information shows the details of SGD calculations for the KRE surface layer.

S.1. SGD derived by three end-members mixing model

Plots of ^{226}Ra and ^{228}Ra activities versus salinity showed that the ^{226}Ra and ^{228}Ra activities in the surface water of the KRE were higher than those expected from a conservative mixing line between Krka River and open seawater (Figure S3). These findings also indicate that there was an excess of Ra entering the estuary from other sources, such as SGD (Moore, 2010; Peterson et al., 2008). Because ^{228}Ra has a shorter half-life than ^{226}Ra, the ^{228}Ra activities in the coastal Adriatic Sea are much lower than those in the estuary, whist differences in ^{226}Ra activities between the coastal Adriatic Sea and the estuary are much smaller. Therefore, using ^{228}Ra to establish the three end-member mixing model is more appropriate due to its lower mixing effect from the coastal sea. Meanwhile, we estimated another ^{228}Ra source that desorbed from the suspended particles. We found that desorbed ^{228}Ra activity in the KRE was considerably lower than that in the seawater (*vide infra* Section S.2). Therefore, a three end-member mixing model was established based on salinity and ^{228}Ra to estimate the fractions of (1) open seawater, (2) river water and (3) groundwater in the KRE surface water.

We used the following equations for the types of water, salinity and ^{228}Ra balance as follows (Moore, 2003):

$$f_S + f_R + f_{GW} = 1 \tag{A.1}$$

$$S_S f_S + S_R f_R + S_{GW} f_{GW} = S_M \tag{A.2}$$

$$^{228}Ra_S f_S + {}^{228}Ra_R f_R + {}^{228}Ra_{GW} f_{GW} = {}^{228}Ra_M \tag{A.3}$$

Here, f refers to the fraction of the open seawater (S), river (R) and groundwater (GW) end-member; S_S, S_R, S_{GW} and $^{228}Ra_S$, $^{228}Ra_R$, $^{228}Ra_{GW}$ are the salinity and ^{228}Ra activity in the open seawater, river and groundwater, respectively. The subscript M represents the measured values of salinity and ^{228}Ra of an individual sample. The equations above can be solved to obtain the fraction of each end-member:

$$f_S = \frac{\left(\frac{^{228}Ra_M - ^{228}Ra_R}{^{228}Ra_{GW} - ^{228}Ra_R}\right) - \left(\frac{S_M - S_R}{S_{GW} - S_R}\right)}{\left(\frac{^{228}Ra_S - ^{228}Ra_R}{^{228}Ra_{GW} - ^{228}Ra_R}\right) - \left(\frac{S_S - S_R}{S_{GW} - S_R}\right)} \quad \text{(A.4)}$$

$$f_{GW} = \frac{S_M - S_R - f_S(S_S - S_R)}{S_{GW} - S_R} \quad \text{(A.5)}$$

$$f_R = 1 - f_S - f_{GW} \quad \text{(A.6)}$$

The three end-member values shown in Figure S3, which were 49±8 dpm m^{-3} (KR13, S=36.9) for open seawater, 33±7 dpm m^{-3} (KR1, S=0.2) for river water and 260±56 dpm m^{-3} (average, S=6.8) for groundwater. Thus, we evaluated the fractions of open seawater, river water and groundwater in the KRE surface water. The results obtained from this model are shown in Figure S4. As expected, in the surface water of the KRE, the fraction of the river water (42±12 %) was higher than the fraction of the open seawater (31±8 %) and groundwater (27±9 %). During the time series observation, a smaller variation range (28-37 %) was observed for the open seawater fraction compared to the variation ranges for the river water and groundwater fractions.

Prior to SGD flux estimation, it was necessary to assess the flushing time of KRE surface layer. Because the KRE is highly stratified, we were interested in computing flushing time mainly for the surface freshwater and brackish layers, which were together approximately 2.5 m deep. In this way, assuming the KRE surface layer water above the halocline was well mixed, we used a method based on a physical model described by Sanford et al. (1992) and Moore et al. (2006) as follows:

$$T_f = \frac{V}{(1-b)Q+I} \quad \text{(A.7)}$$

Here, T_f is the flushing time, V refers to the volume of the surface estuarine water layer, which is defined as the product of the average area and depth, $Q=P/T$, where T is the tidal period and P is the tidal prism, b represents the return flow into the coastal sea from the study region, and I is the net inflow of the Krka River into the KRE during the sampling period. In the studied estuary, the regular semidiurnal tidal period was approximately 0.47 days as determined by the time series observation. The tidal prism *P* can be determined by multiplying the average surface area by the tidal range during the sampling period, which was estimated to be 2.6×10^6 m^3. In this model, *b* is equivalent to the open seawater fraction, while the fraction of open seawater calculated above represents only the surface water. Based on the salinity profiles of the KRE surface layer water, we calculated the fraction of open seawater in the total surface layer water (up to the depth of 2.5 m) of the KRE to be 0.49±0.21. Therefore, the estimated flushing time of the KRE surface layer water was 2.8±1.2 days. Of note, the flushing time calculated in this study was obtained from only a part of the KRE brackish water (within blue dashed line in Figure 1), whereas the reported flushing time of the whole KRE brackish water was approximately 20 days in September (Legović, 1991). In our study, the river flow is much greater and the volume of analyzed water for the flushing time is smaller compared to the conditions presented by Legović (1991) for September. Legović (1991) also does not include the impact of SGD, which should reduce the flushing time of the upper layer above the halocline in the KRE. Therefore, these factors (i.e. flow rate, water volume above the halocline, and impact of SGD) could have contributed to the shorter flushing time reported in this study.

Based on the three end-member mixing model, we also calculated the fraction of groundwater in the estuary to be 0.20±0.07. Assuming this value represents the fraction of groundwater in the KRE surface layer of our study, we can obtain the flux of SGD by using the following equation:

$$SGD = \frac{Vf_{GW}}{T_f} \tag{A.8}$$

Therefore, the flux of SGD into the KRE surface layer was calculated to be (6.5-26.7) × 10^5 m^3 d^{-1}, with an average of 16.2 × 10^5 m^3 d^{-1}.

S.2. SGD derived from Ra mass balance model

Generally, in a defined system with a presumed steady state, the Ra mass balance is equal to the sum of inputs (which are usually from river supply, sediments diffusion and SGD) and the outputs/loss (which include open seawater mixing and Ra decay) (Moore, 1996; Moore et al., 2006). Based on these facts, the Ra mass balance model is another approach to quantify the magnitude of SGD. This model has been widely applied to estuaries around the world (Liu et al., 2017; Moore et al., 2008; Rengarajan and Sarma, 2015). We carried out a mass balance model of ^{228}Ra to estimate the SGD flux in the KRE surface layer (Figure S5). The existence of a permanent halocline in the KRE could prevent ^{228}Ra diffusion from the sediments through the halocline into the surface layer water and therefore the term of sediment diffusion was disregarded. Atmospheric deposition was also eliminated because it is negligible.

We formulated Eq. (A.9) for the ^{228}Ra mass balance model in the KRE surface layer as follows:

$$F(^{228}Ra_{river}) + F(^{228}Ra_{susp}) + F(^{228}Ra_{SGD}) = F(^{228}Ra_{mix}) \quad \text{(A.9)}$$

Here, $^{228}Ra_{river}$, $^{228}Ra_{susp}$ and $^{228}Ra_{SGD}$ represent the ^{228}Ra flux input from the Krka River, suspended particles and SGD, respectively; and $^{228}Ra_{mix}$ represents the ^{228}Ra loss by mixing with the open seawater. Then, SGD-derived ^{228}Ra flux and SGD flux into the KRE surface layer can be obtained by Eq. (A.10) and Eq. (A.11):

$$\begin{aligned} &F(^{228}Ra_{SGD}) \\ &= [C(^{228}Ra_{ES}) - f_S \times C(^{228}Ra_{SW}) - C(^{228}Ra_{susp})] \times A_{ES} \times H_{upper} \times (1/T_f) - C(^{228}Ra_{river}) \times F_{river} \end{aligned} \quad \text{(A.10)}$$

$$Q_{SGD} = \frac{F(^{228}Ra_{SGD})}{C(^{228}Ra_{gw})} \quad \text{(A.11)}$$

Here, $C(^{228}Ra_{ES})$, $C(^{228}Ra_{SW})$, $C(^{228}Ra_{susp})$, $C(^{228}Ra_{river})$ and $C(^{228}Ra_{gw})$ are the ^{228}Ra activity in the KRE surface layer, open seawater, suspended particles, the Krka River and groundwater, respectively. A_{ES} and H_{upper} are the area and depth of the KRE surface layer (2.5 m), respectively. F_{river} is the Krka River flow (i.e. discharge) during the sampling period. In this study, the desorption of ^{228}Ra activity from suspended particles was calculated from the equation $A=A_{susp}\times SPM\times f$, where A_{susp} is the ^{228}Ra activity from the suspended particles. We used the maximum ^{228}Ra activity in the surface sediment which is 1.0 dpm g^{-1} (Cukrov and Barišić, 2006). *SPM* is the concentration of suspended particles in our study area and we used the highest value of 6.0 g m^{-3} (Cindrić et al., 2015); *f* is the maximum ^{228}Ra desorption fraction of 0.38 (Gu et al., 2012). Thus, ^{228}Ra activity desorbed from suspended particles in the KRE surface layer was estimated to be 2.3 dpm m^{-3}, which was considerably lower than ^{228}Ra activity (100 dpm m^{-3}) in the estuarine water. Based on Eqs. (A.10) and (A.11), we determined the SGD flux in the KRE surface layer to be (4.7-21.0) × 10^5

$m^3\ d^{-1}$, with an average of $12.8 \times 10^5\ m^3\ d^{-1}$. The definitions and values of parameters are summarized in Table S1.

S.3. Tidal effects on SGD

We employed a method based on the Ra activity from the time series observation of tidal cycles to evaluate the tidal pumping effect on SGD flux in the KRE surface layer. Following the approach of Peterson et al. (2008) and Wang and Du (2016), the SGD flux was calculated using Eq. (12):

$$Q_{SGD} = \frac{(Ra_{total} - Ra_{bkgd}) \times A_{ES} \times H_{upper}}{T_f \times Ra_{gw}} \qquad \text{(A.12)}$$

Here, we used the following steps to evaluate the SGD flux:

i) Since each measured Ra activity (Ra_{total}) in the KRE surface layer was the result of total Ra sources, we calibrated each measured Ra activity by subtracting the estuarine background Ra activity (Ra_{bkgd}) from Ra_{total}. We chose the minimum activity from measured values in the time series observation as the background of estuarine water for a conservative SGD estimation. In this way, we could conclude that the excess Ra activity came exclusively from SGD.

ii) Assuming that the Ra activity in time series observation can represent the Ra activity in the KRE surface layer, we estimated the excess Ra inventory by multiplying excess Ra activity by the KRE surface layer depth (H_{upper}, 2.5m) and the studied estuarine area (A_{ES}, $9.3 \times 10^6\ m^2$).

iii) The excess Ra inventory is divided by the estimated flushing time of the surface estuarine water (T_f, 2.8 days) to obtain Ra flux only from SGD.

iv) Finally, after dividing the Ra flux by the Ra activity in the groundwater end-member (Ra_{gw}), which was 260 ± 56 dpm m^{-3} for ^{228}Ra, we obtained the SGD flux in the KRE surface layer (Q_{SGD}).

Therefore, based on the Ra activities in time series observation and by applying Eq. (A.12), we were able to determine the SGD flux for each time series sample as shown in Figure S6, suggesting a clear hysteresis effect. The range of SGD fluxes in the KRE surface layer during the tidal cycles was $(3.2\text{-}18.1) \times 10^5\ m^3\ d^{-1}$ with an average of $7.8 \times 10^5\ m^3\ d^{-1}$.

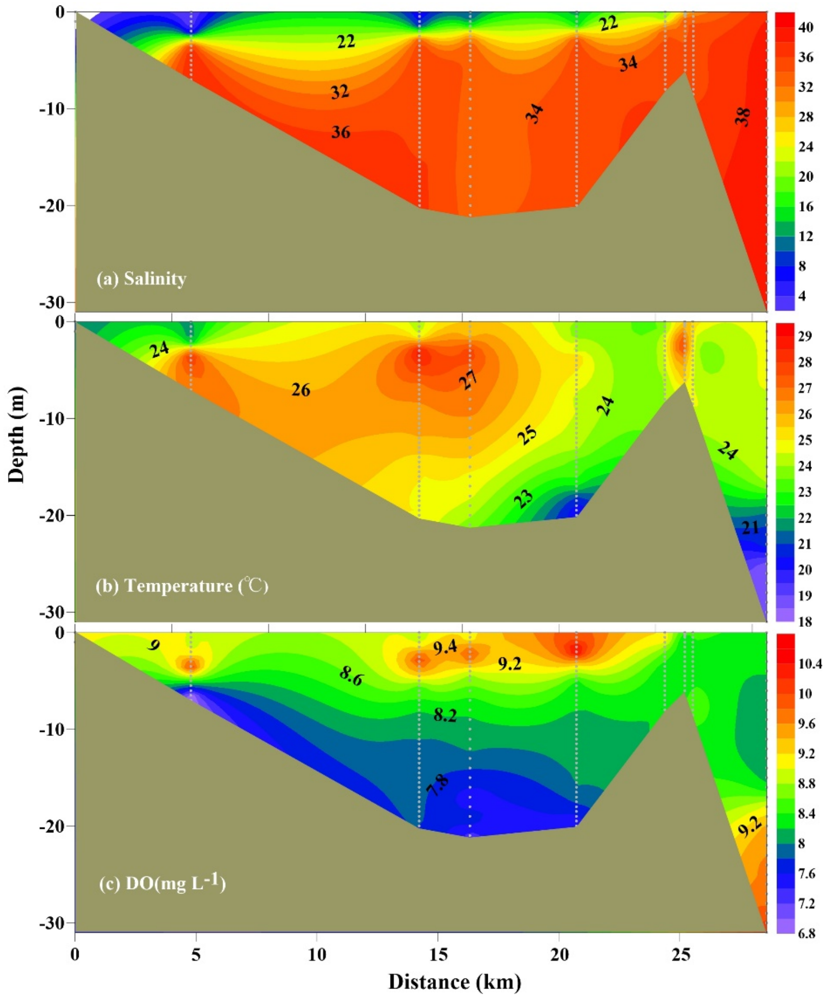

Figure S1. Vertical distributions of (a) salinity, (b) temperature and (c) dissolved oxygen (DO) from Krka River, along the estuary up to the Adriatic Sea. Dotted lines represent hydrological data of all samples. The X-axis is the distance from the end-member of freshwater.

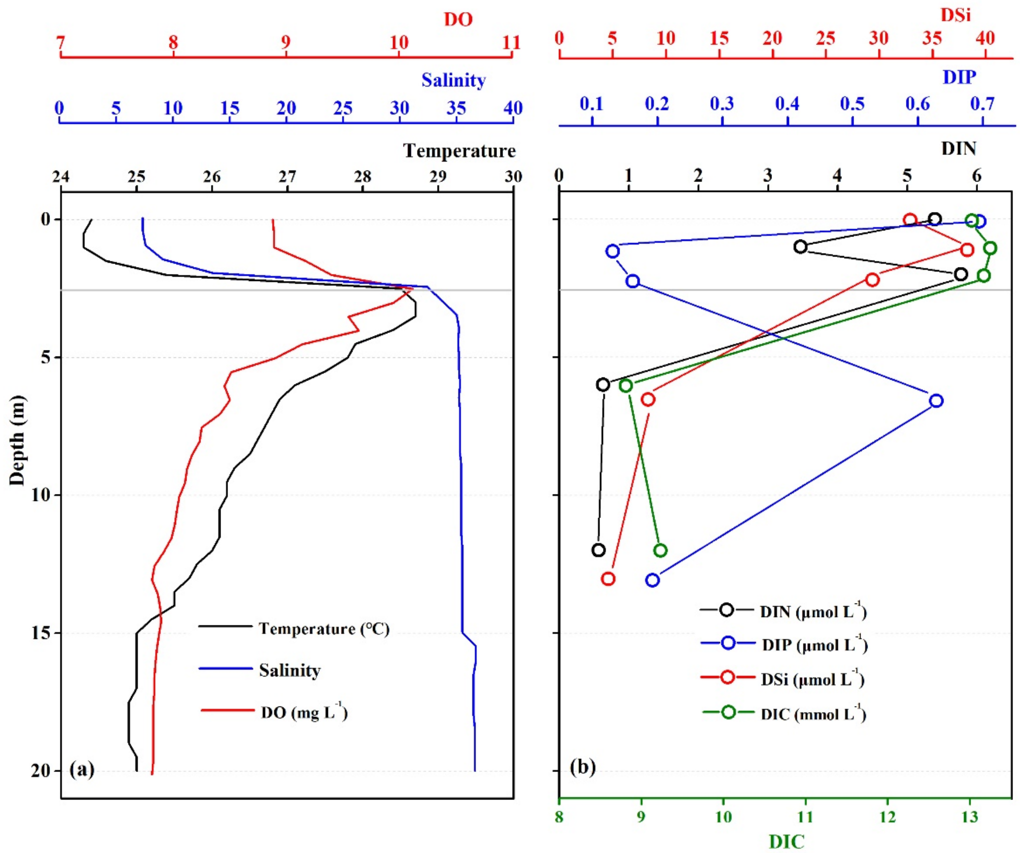

Figure S2. Vertical profiles of (a) hydrological parameters and (b) nutrient and DIC concentrations for station KR3.

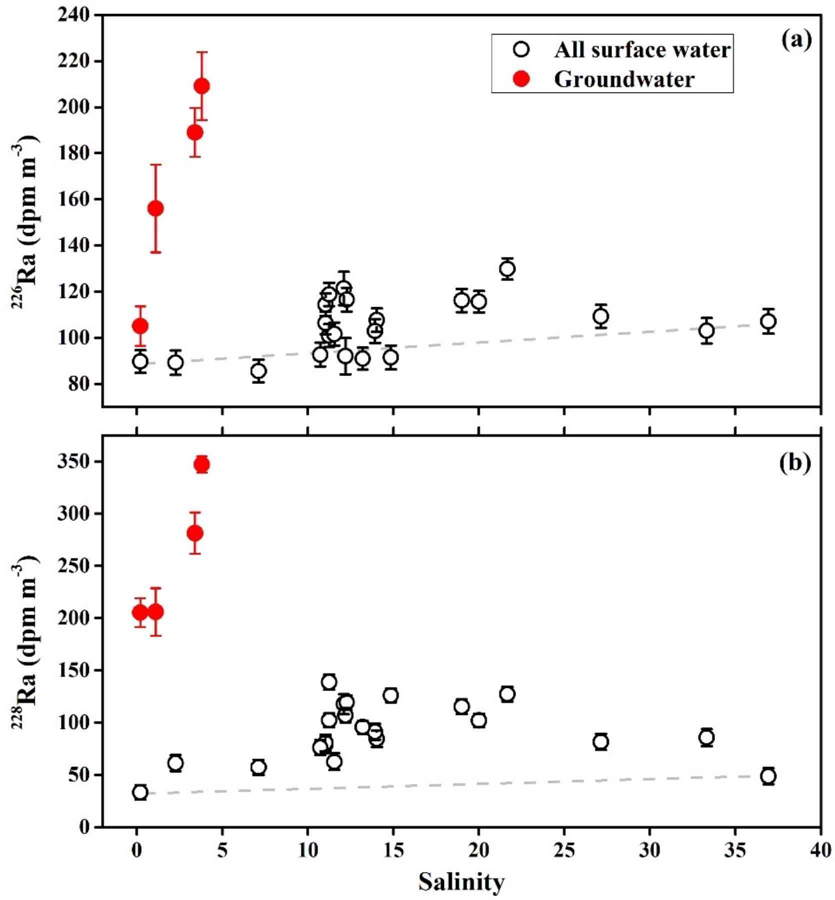

Figure S3. Plots of (a) ^{226}Ra and (b) ^{228}Ra activities versus salinity in the surface water (including time series observation) and groundwater of the KRE. Dashed lines represent the expected conservative mixing between Krka River freshwater and open seawater.

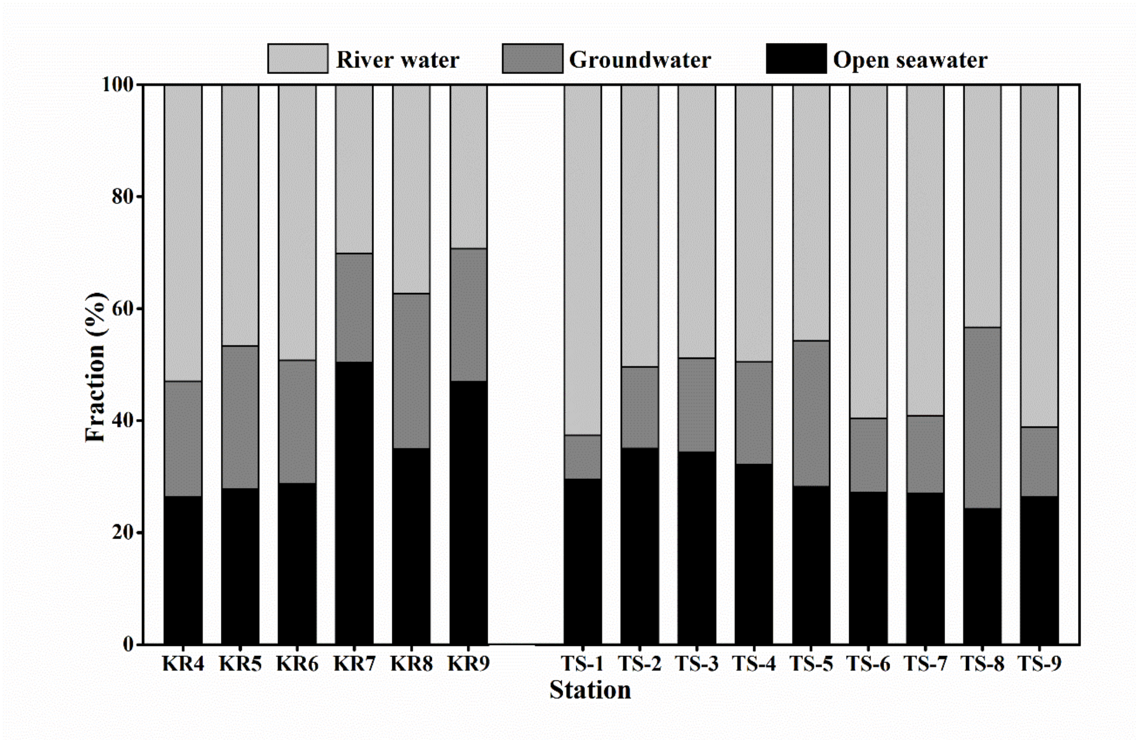

Figure S4. Fractions of groundwater, river water and open seawater in the surface water of KRE.

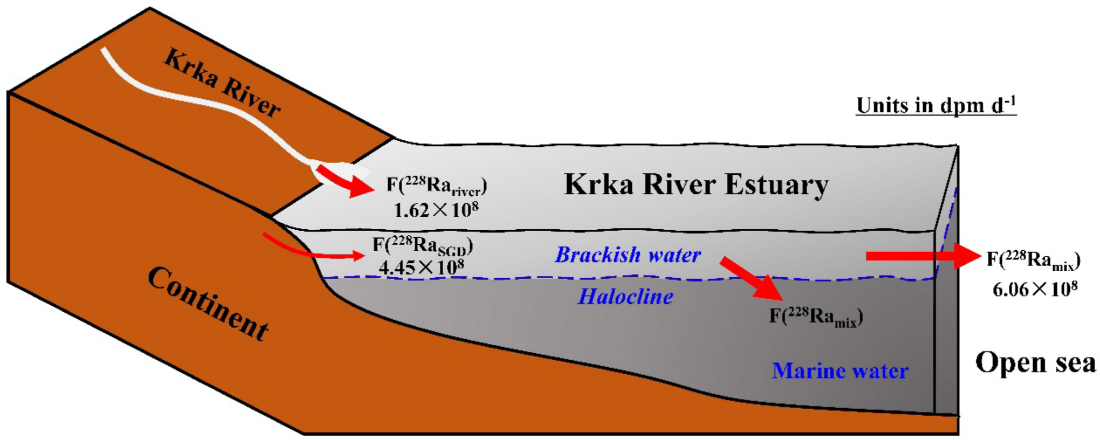

Figure S5. A schematic depiction of ^{228}Ra mass balance (dpm d^{-1}) in the KRE surface layer.

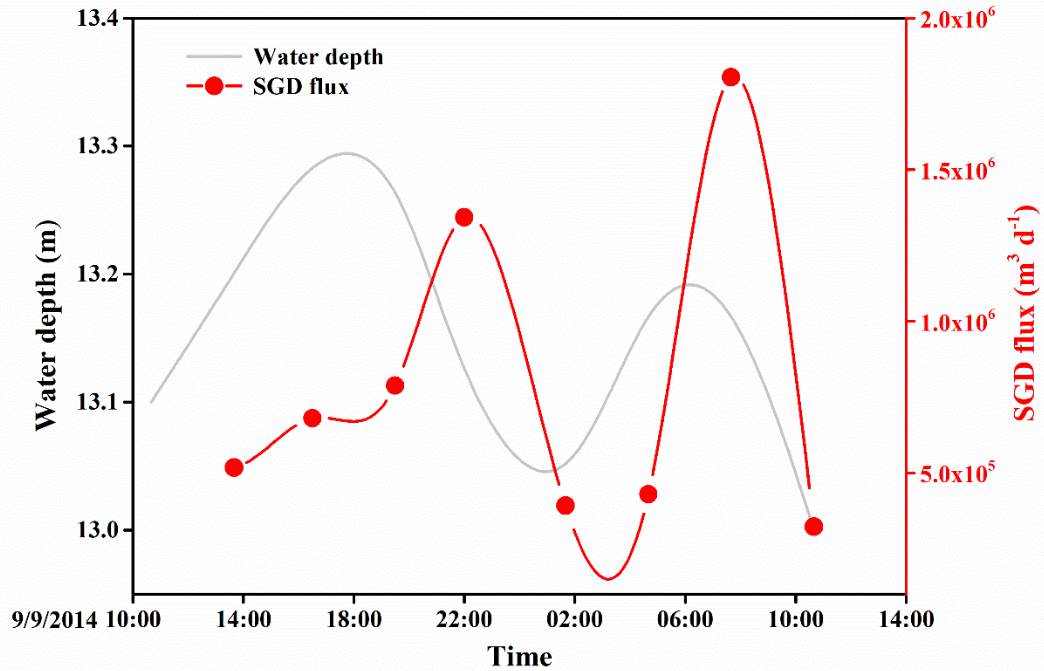

Figure S6. SGD flux and water depth variations during the tidal cycles.

Table S1. Definitions and values of parameters used in the equations for ^{228}Ra mass balance and calculations of SGD flux in the KRE surface layer.

Parameter	**Definition**	**Value**	**Unit**
$^{228}Ra_{ES}$	^{228}Ra activity in the KRE surface layer	100 ± 20	dpm m^{-3}
$^{228}Ra_{SW}$	^{228}Ra end-member in the open seawater	49 ± 8	dpm m^{-3}
$^{228}Ra_{susp}$	^{228}Ra activity desorbed from suspended particles	2.3	dpm m^{-3}
$^{228}Ra_{river}$	^{228}Ra end-member in the Krka River water	33 ± 7	dpm m^{-3}
$^{228}Ra_{gw}$	^{228}Ra end-member in the groundwater	347 ± 8	dpm m^{-3}
A_{ES}	Surface area of the KRE	9.3×10^6	m^2
H_{upper}	Water depth of the KRE	2.5	m
T_f	Measured flushing time in the KRE surface layer	2.8 ± 1.3	d
F_{river}	Krka River freshwater discharge	4.8×10^6	m^3 d^{-1}